CONF-9009294--1

DE91 004474

DEC 0 4 1990

TWO-ELECTRON EXCITATION IN SLOW ION-ATOM COLLISIONS: EXCITATION MECHANISMS AND INTERFERENCES AMONG AUTOIONIZING STATES

M. Kimura

Argonne National Laboratory, Argonne, IL 60439, and
Dept. of Physics, Rice University, Houston, TX 77251

ABSTRACT

The two-electron capture or excitation process resulting from collisions of H^+ and O^{6+} ions with He atoms in the energy range from 0.5 keV/amu to 5 keV/amu is studied within a molecular representation. The collision dynamics for formation of doubly excited O^{4+} ions and He^{**} atoms and their $(n\ell, n'\ell')$ populations are analyzed in conjunction with electron correlations. Autoionizing states thus formed decay through the Auger process. An experimental study of an ejected electron energy spectrum shows ample structures in addition to two characteristic peaks that are identified by atomic and molecular autoionizations. These structures are attributable to various interferences among electronic states and trajectories. We examine the dominant sources of the interferences.

I. INTRODUCTION

Recent measurements of the ejected electron energy spectrum (EEES) resulting from collisions of ions with He atoms at low to intermediate energies have been made by using (i) multiply charged ion projectiles [1,2] such as O^{6+} and C^{6+} and (ii) singly charged ion projectiles [3,4] such as H^+ and Li^+. These measurements have revealed an interesting pattern of interferences in the EEES and a signature of electron correlation. For multiply charged ions, doubly excited states of the projectile are produced through multiple-electron capture. In contrast, target double excitation is dominant for singly charged ions. Hence, the two-electron excitation mechanism is significantly different for these projectiles. This fact certainly affects two-electron $(n\ell m, n'\ell' m')$ distribution. Here $(n\ell m)$ designates a set of quantum numbers of an atomic state, principal, angular, and magnetic, respectively. The electron correlation effect may play a role in assigning a seat for each electron during a collision. The contribution, if any, of this effect is an important topic to investigate.

The interaction time for a collision system of, for example, H^+ + He below several keV has a lifetime of approximately the same order as various doubly excited states of the He atom. Therefore, the doubly excited states produced by such a

DISTRIBUTION OF THIS DOCUMENT IS UNLIMITED

The submitted manuscript has been authored by a contractor of the U. S. Government under contract No. W-31-109-ENG-38. Accordingly, the U. S. Government retains a nonexclusive, royalty-free license to publish

MASTER

collision decay through the Auger process by ejecting a continuum electron while the projectile is still near. Hence, the ejected electron feels all interactions from a colliding system, including electron-electron interaction, and is influenced by Coulomb interaction of the projectile or by postcollision interactions (PCI). Consequently, the energy and angular distributions of the ejected electron are broadened and shifted and show a variety of structures that are due to interferences arising from various sources.

In this report, we summarize our current understanding of two-electron excitation dynamics and the origins of structures seen in the EEES that result from collisions of multiply and singly charged ions with He atoms in the energy regions from 0.5 keV/amu to 5 keV/amu.

II. TOOLS FOR ANALYSIS

A molecular orbital (MO) expansion method [5] within a semiclassical representation is considered to be one of the most appropriate treatments for the collisions considered here. Therefore, we adopted the method for systematic analysis and understanding of the experimental results. Minimal information about the method that is necessary for later discussions is provided here. Readers can find a more comprehensive description elsewhere [5].

A. Molecular States

1. Discrete states. A two-electron configuration interaction (CI) method modified by the inclusion of a pseudopotential was used to obtain discrete molecular states including doubly excited states. Slater-type orbitals were used to construct basis sets. The typical number of configurations for a two-electron system in the present calculation ranges from 150 to 250.

2. Continuum states. The continuum state was obtained by numerically solving the Hartree-Fock (HF; exact static-exchange) approximation for elastic electron scattering from the molecular ion. Autoionization rates based on the static-exchange HF approximation and Coulomb wavefunctions are in good accord if the same molecular ion potential is used [6]. Hence, the Coulomb continuum state was also employed in the present study.

B. Scattering Dynamics

1. Coupled equations. The total scattering wavefunction is expanded in terms of discrete and continuum states as

$$\psi(\vec{r},t)=\sum_i a_i(t)\phi_i^{MO}(\vec{r},\vec{R})F_i(\vec{r},\vec{R},t)$$

$$+\sum_{\ell m}\int d\varepsilon\, b_{\varepsilon\ell m}(t)\phi_{\varepsilon\ell m}^{MO}(\vec{r},\vec{R})F_\varepsilon(\vec{r},\vec{R},t), \qquad (1)$$

where $\phi_j^{MO}(\vec{r},\vec{R})$ represents discrete or continuum molecular electronic wavefunctions with a representative set of quantum designation j, and $F_j(\vec{r},\vec{R},t)$ contains all phase factors as well as electron translation factors (ETFs) [5]. The first term of Eq. (1) represents a set of discrete states and the second a set of continuum states. The integral over the ejected electron energy ε in the second term is evaluated by discrete sampling at a variety of discrete energies (by discretization). Substituting Eq. (1)

into the time-dependent Schrödinger equation with assumption of a well-defined trajectory for heavy particle motion [5] gives a set of first-order, time-dependent coupled equations,

$$\begin{bmatrix} \dot{a}_i \\ \dot{b}_{\varepsilon\ell m} \end{bmatrix} = \sum_{j,\varepsilon'\ell'm'} \begin{bmatrix} U_{i,j} & U_{i,\varepsilon'\ell'm'} \\ U_{\varepsilon\ell m,j} & U_{\varepsilon\ell m,\varepsilon'\ell'm'} \end{bmatrix} \begin{bmatrix} a_j \\ b_{\varepsilon'\ell'm'} \end{bmatrix}, \tag{2}$$

where $V_{i,j}$, $V_{i,\varepsilon'\ell'm'}$, and $V_{\varepsilon\ell m,\varepsilon'\ell'm'}$ represent discrete-discrete, discrete-continuum, and continuum-continuum couplings, respectively, and are given in general form as

$$U_{kn} = \left\langle k \left| H_{e\ell} - i\frac{\partial}{\partial t} \right| n \right\rangle. \tag{3}$$

$H_{e\ell}$ and $\frac{\partial}{\partial t}$ denote the electronic Hamiltonian and nuclear momentum, respectively. $|k\rangle$ is the k^{th} molecular state.

2. Dynamical couplings

a. discrete-discrete couplings. Nonadiabatic couplings arising from nuclear motion [the second term in Eq. (3)] cause electronic transitions of the colliding system. These nonadiabatic couplings can be separated into two different contributions, namely radial and angular (rotational) couplings depending on the nuclear motion,

$$U_{ij} = \dot{R}\left\langle i \left| -i\frac{\partial}{\partial R} \right| j \right\rangle + \dot{\vartheta}\left\langle i \left| iL_y \right| j \right\rangle + \text{(ETF terms)}. \tag{4}$$

Here $\dot{R}$ and $\dot{\vartheta}$ represent radial and angular velocities, respectively, and iL_y is the electronic orbital angular momentum component perpendicular to the collision plane. As is frequently discussed [7], the nonadiabatic couplings have inherent defects that cause serious problems in the scattering equation. The ETFs correct those defects by satisfying correct scattering boundary conditions.

b. discrete-continuum couplings. Phenomenologically, the possibility of transitions to the ionized continuum can be described by a complex optical potential. The imaginary part of the potential gives rise to the absorption of the initial atoms, i.e., ionization. This imaginary part represents the autoionization width [the first term in Eq. (3)] and can be approximated by

$$\Gamma(R) = 2\pi \sum_{\ell m} \left| \left\langle \mathcal{A}\phi_j^{AB^+}(\vec{r},\vec{R})\varphi_{\varepsilon\ell m}^{e^-} \left| H_{e\ell} \right| \phi_i^{AB^*}(\vec{r},\vec{R}) \right\rangle \right|^2 \rho_\varepsilon, \tag{5}$$

where $\phi_i^{AB^*}$ and $\phi_j^{AB^+}$ $\varphi_{\varepsilon\ell m}^{e^-}$ represent a doubly excited autoionizing state and ionized state, respectively, and are assumed to be orthogonal. ρ_ε is the density of the state, and $\mathcal{A}$ is the antisymmetrizer.

III. REPRESENTATIVE CASES

A. Excitation Mechanism

As discussed, the two-electron excitation mechanisms for the multiply charged ion and the singly charged ion projectile are significantly different. It is convenient to discuss them separately.

1. Multiply charged ions -- He. Figure 1 illustrates typical adiabatic potentials for this case for the C^{4+} + He system as an example. Important characteristics of the potentials are the following: (i) closely lying single-electron and double-electron capture states, (ii) a strong mixing of states of higher M_L because of a large n-manifold contribution to capture, and (iii) a series of narrow avoided crossings between the initial channel and the electron capture states with large (n, ℓ) values. These features clearly indicate that electron capture proceeds by both single and double capture processes through a combination of successive radial and rotational couplings leading to high (nℓm) states. For a flux exit from the initial channel, the position of the avoided crossing and the corresponding energy splitting (the reaction window) primarily govern the electron capture dynamics, mainly through a strong radial coupling. On the outgoing paths of collisions, flux redistribution takes place within the same n-manifold, populating higher ℓ and m states as a result of strong rotational coupling.

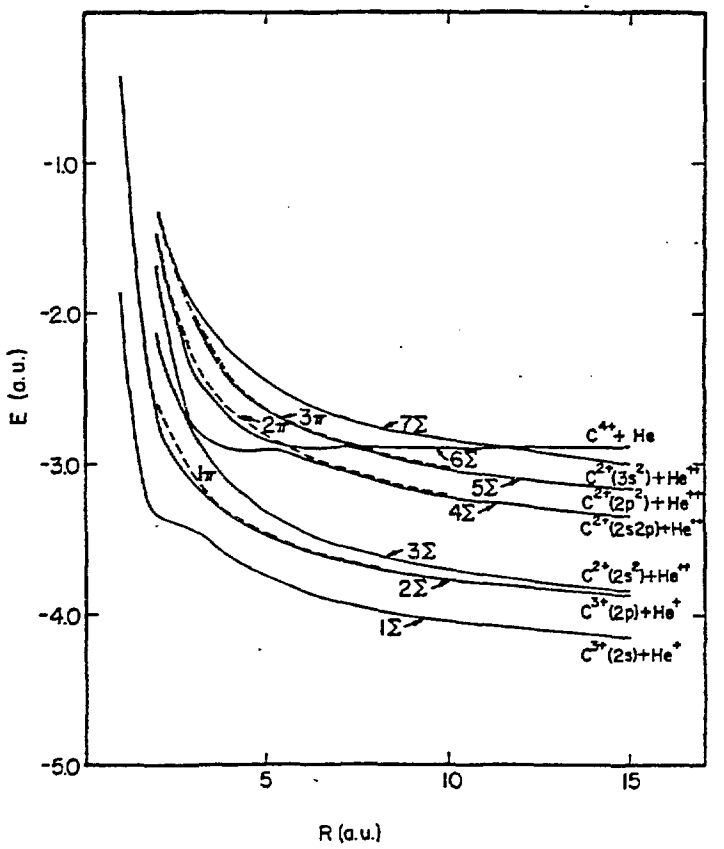

Fig. 1. Adiabatic potentials for C^{4+} + He system.

A recent experiment [8] by Stolterfoht et al. produced evidence of an electron correlation effect for two-electron capture. The authors observed Coster-Kronig electrons [one electron in a low-n (≅3) manifold and another in a high-n (≥6) manifold] along with the usual LMM Auger electrons ($n\ell$, $n\ell'$) in O^{6+} + He collisions at E = 60 keV. This experiment may shed some light on electron correlation during a collision (dynamical electron correlation). Figures 2 and 3 display recent theoretical results obtained by using the MO treatment [9] for n and m distributions for the O^{6+} + He collision system at 60 keV along with the measured data of Stolterfoht et al. [8]. As suggested at the beginning of this section, the population of the m-distribution covers a wide range of m values with a peak at m=2,3. This is a direct consequence of strong mixing of the flux within n-manifold through long-range rotational coupling at the outer part of the collision. The trend of the n-distribution can be interpreted by using the argument of a reaction window. Although the (n=2, n'=12) manifold crosses the initial channel at larger R (internuclear separation) than does the (n=2, n'=6) manifold, the crossing of the latter is more effective for electron capture and results in a larger population for the (n=2, n'=6) manifold. For the dynamical electron correlation the effect is rather difficult to identify because the transitions to both the Coster-Kronig and LMM Auger levels are due to "conventional" curve crossings in the MO study. More extensive and systematic studies on the topic would certainly provide a more detailed understanding of underlying collision physics.

2. Singly charged ions -- He. Figure 4 depicts a typical example of adiabatic potentials for a singly charged ion, with the H^+ + He system as an example. In contrast to the previous case, all doubly excited states arise solely from the target He atom. Furthermore, no apparent avoided crossings exist, at least among low-lying single-electron excitation/capture states. All doubly excited states of He lie above and well separated from the single-electron channels. Hence, this case requires a ladder-climbing mechanism for electrons to be promoted to doubly excited states from the ground level. In such a mechanism, a strong rotational coupling at the united-atom limit (R=0) usually plays a key role in the electron promotion. For example, Fig. 4 shows that subsequent two-step rotational couplings proceed by flux promotion from

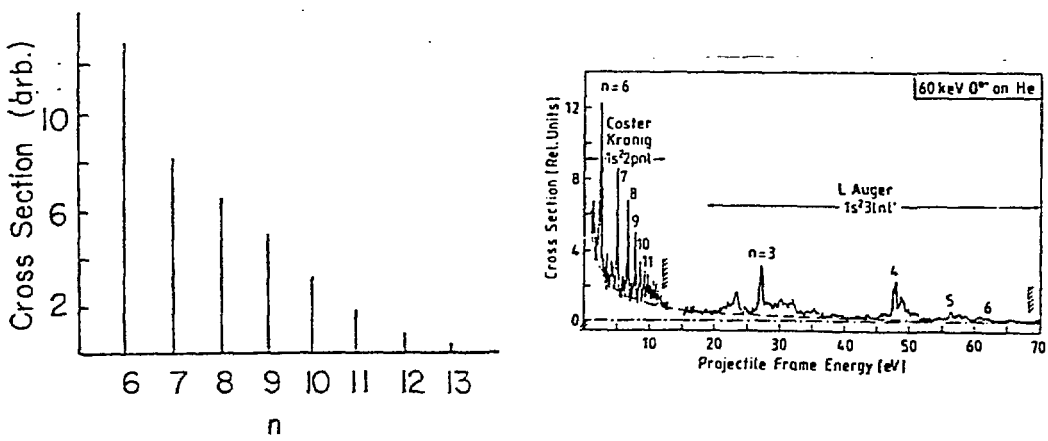

Fig. 2. n distribution in O^{6+} + He collisions at 60 keV.
Left panel: theory
Right panel: experiment (Ref. 8)

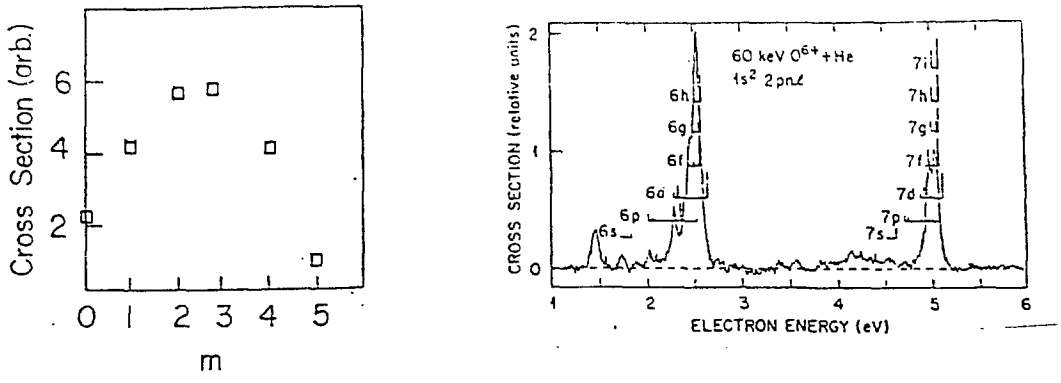

Fig.3. m distribution in O^{6+} + He collisions at 60 keV.
Left panel: theory
Right panel: experiment

the ground H^+ + He state to the single-excitation H^+ + He(1s2p) state and to the double-excitation H^+ + He($2p^2$ ^1D) state. In addition, Demkov-type radial coupling plays another role in flux promotion between states with the same symmetry. Demkov coupling is partly responsible for production of the He($2s^2$ ^1S) state through weak radial coupling directly from the ground state. As Fig. 4 shows, doubly excited states, unlike low-lying states, are densely packed within a narrow energy band with ample sharp avoided crossings in a wide range of R values, and vigorous flux exchange among them can be expected in both incoming and outgoing collision paths. This may cause some interference patterns in the EEES, as we will see in the next section.

B. Ejected Electron Energy Spectrum

Doubly excited states decay through the Auger process by emitting a continuum electron. Interference arising from flux exchange among states and trajectory effects is expected to affect energy and angular distributions of the continuum electron, causing structures in the EEES. Analysis of these structures deepens our understanding of collision dynamics and atomic/molecular structure.

Inspection of the potentials for the H^+ + He system in Fig. 4 indicates possible sources of interference that should be examined [10]. These sources are the interferences between (i) M_L states in a single ($n\ell$, $n'\ell'$) manifold, (ii) nearby autoionizing states (doubly excited He channels and Penning channels), (iii) different atoms in a symmetric system, (iv) direct ionization and autoionization, (v) autoionization in incoming and outgoing parts of a collision, (vi) different paths, and (vii) different locations on a single path with the same ejected electron energy. Sources (v)-(vii) lead to interferences because the phase factors evolve differently in time, at different R values. In addition, experimental evidence has been a reported for interaction between an electron ejected by the Penning process and the nuclear motion of a residual molecular ion [11]. The interference was caused by an exchange of

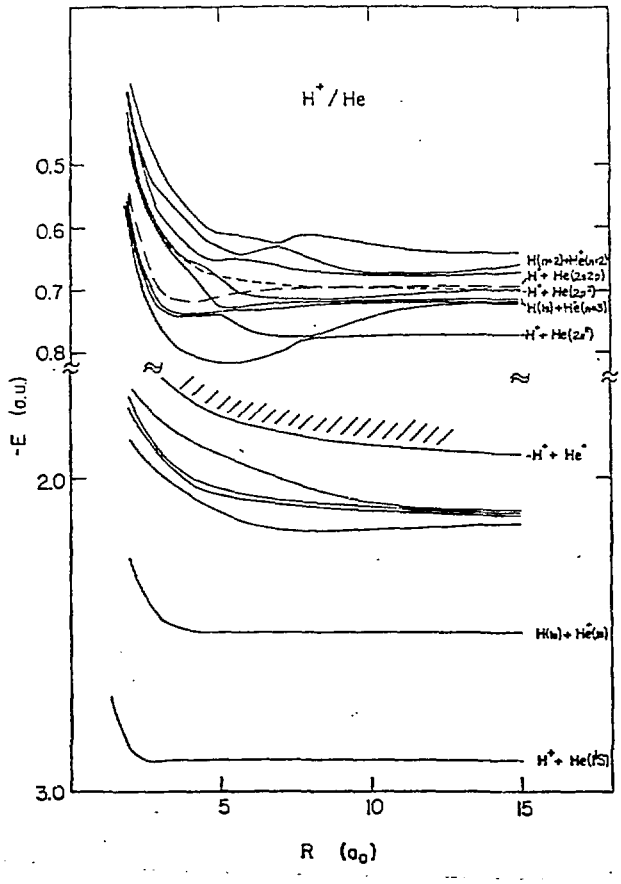

Fig. 4. Adiabatic potentials for H^+ + He system.

angular momentum in the high-meV collision regime. However, in the present study, we excluded this possibility because the energy region of our interest is far higher than that of the experiment. We also neglected (iii) because our test system is not symmetric. We examined possible sources (i)-(vii), with the exception of (iii), and their relative importance.

Figure 5 shows the EEES obtained by fully accounting for (i)-(vii). The general features of the EEES are (i) the dominant peaks at $\varepsilon \cong 35$ eV and 33 eV that are due to atomic autoionization (AAI) of the He atom, (ii) the broad peak between 33 eV and 35 eV that is due to molecular autoionization (MAI) from the HHe^+ quasimolecule, and (iii) the PCI effect and the Doppler shift on the lower energy side. Helium doubly excited states for $2s^2\ ^1S$, $2p^2\ ^1D$, and $2s2p\ ^1P$ are considered to be the prime channels for excitation. Their nominal energies are 33.2 eV, 35.30 eV, and 35.54 eV, respectively, and their lifetimes [12] are known to be in the ranges of 4×10^{-15} sec, 9×10^{-15} sec, and 15×10^{-15} sec, respectively. Hence, at the higher energy end of the present study, a combination of $2s2p\ ^1P$ and $2p^2\ ^1D$ autoionizing states is primarily responsible for the AAI peak. The $2s^2\ ^1S$ state with the PCI effect and the Doppler shift tailing from two levels above cause the broad MAI peak. As the energy decreases, one would expect the AAI peak to decrease and merge with the MAI peak to form a broad peak with abundant structures. The transition probability, I_{fi}, for autoionization is described in a coherent sum of amplitudes, written in a simplified form as

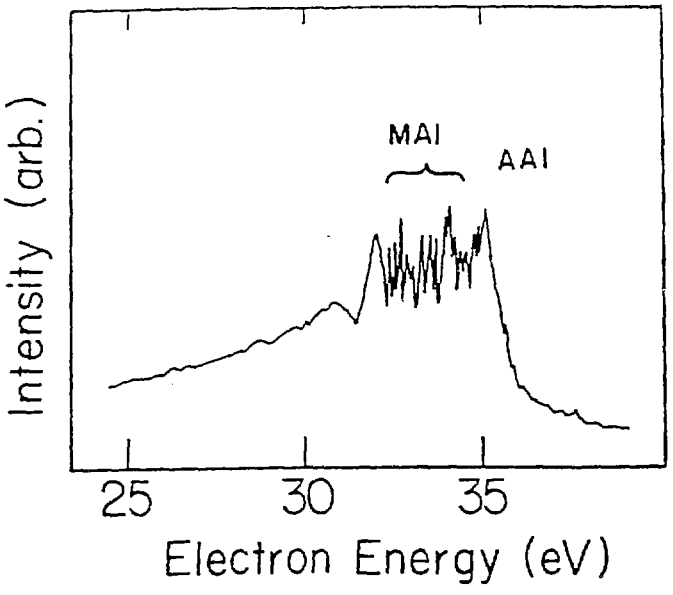

Fig. 5. The ejected electron energy spectrum resulting from H^+ + He collisions at 0.8 keV.

$$I_n \alpha \left| \Sigma_L A_L(t) g_{PCI}(\varepsilon_L, \varepsilon, D) V_{\varepsilon d} Y_L(\Omega) \right|^2, \qquad (6)$$

where $A_L(t)$ describes the transition amplitude for forming a doubly excited state with the representative quantum state L of the He atom, and g_{PCI} (ε_L, ε, D) represents the PCI effect that describes the energy shift of an ejected electron from the nominal energy ε_L to ε and the Doppler shift D caused by the moving, doubly excited He atom. The term $V_{\varepsilon d}$ represents the coupling matrix element between the autoionizing state and the ionized state (the HHe^{2+} core + one free electron), and $Y_L(\Omega)$ denotes all angular components of the ejected electron. Equation (6) qualitatively predicts that the various types of interferences in the EEES for the present collision system originate in the sources summarized as (i)-(vii) above.

The small structures seen between and on the AAI and MAI peaks are due to the causes discussed above. These causes were found to be more sensitive to the autoionization collision energy and impact parameter than to the collision energy and impact parameter for discrete transitions. However, at the lower end of the energy studied (0.5 keV), sources (ii), (vi), and (vii) appear to be dominant contributors to the structures in the EEES.

IV. CONCLUDING REMARKS

The study of formation and decay of doubly excited states resulting from ion-atom collisions has been one of the central subjects in atomic physics in the past few years because several types of accurate coincident measurements have become possible. Understanding the results require a wide knowledge not only of collision dynamics, but also of atomic structures. Unfortunately, theoretical attempts to solve the problem lag behind experimental attempts mainly because of the involvement of electronic continuum states in the theory. Only recently have some preliminary attempts at analysis been made. The present results, based on a calculation with a

small basis set, seem to be promising. More systematic studies using a larger basis set would certainly be desirable.

ACKNOWLEDGEMENTS

This work was supported in part by the U.S. Department of Energy, Assistant Secretary for Energy Research, Office of Health and Environmental Research, under Contract W-31-109-Eng-38. The author is grateful for the organizing committee for the invitation to participate in SPIG-90 and the warm hospitality that was shown during his stay in Yugoslavia. The travel grant by the U.S. National Science Foundation U.S./Yugoslavia Cooperative Research is also appreciated.

REFERENCES

[1] F. W. Meyer, D. C. Griffin, C. C. Havener, M. S. Huq, R. A. Phaneuf, J. K. Swenson, and N. Stolterfoht, In Electronic and Atomic Collisions (N. Holland, Amsterdam, 1988) 673.
[2] P. Roncin, M. Barat, M. N. Gaboriaud, L. Guillemot, and H. Laurant, J. Phys. B 22, (1989) 509.
[3] P. van der Straten, R. Morgenstern, and A. Niehaus, J. Phys. B 21, (1988) 1573.
[4] M. Furune, F. Koike, and A. Yagishita, J. Phys. B 16, (1983) 2539.
[5] M. Kimura and N. F. Lane, Adv. At. Mol. Opt. Phys. 26, (1989) 79.
[6] S. Hara and H. Sato, J. Phys. B 17, (1984) 4301.
[7] J. B. Delos, Rev. Mod. Phys. 53 (1983) 287.
[8] N. Stolterfoht, C. C. Havener, R. A. Phaneuf, J. K. Swenson, S. M. Shafroth, and F. W. Meyer, Phys. Rev. Lett. 58, (1987) 958.
[9] M. Kimura, unpublished.
[10] M. Kimura, H. Sato, and M. Matsuzawa, Nucl. Instrum. and Methods XX, (1991) XXX.
[11] A. Merz, M. W. Müller, M. W. Ruf, H. Hotop, W. Meyer, and M. Movre, Chem. Phys. Lett. 160, (1989) 377.
[12] W. Shearer-Izumi, At. Data and Nucl. Tables 20, (1977) 531.

DISCLAIMER

This report was prepared as an account of work sponsored by an agency of the United States Government. Neither the United States Government nor any agency thereof, nor any of their employees, makes any warranty, express or implied, or assumes any legal liability or responsibility for the accuracy, completeness, or usefulness of any information, apparatus, product, or process disclosed, or represents that its use would not infringe privately owned rights. Reference herein to any specific commercial product, process, or service by trade name, trademark, manufacturer, or otherwise does not necessarily constitute or imply its endorsement, recommendation, or favoring by the United States Government or any agency thereof. The views and opinions of authors expressed herein do not necessarily state or reflect those of the United States Government or any agency thereof.

SVEN